*Science Progress (2001), 84 (1), 45–68*

# Use of EPR spectroscopy to study macromolecular structure and function

*ROOPA BISWAS, HENRIETTE KÜHNE, GARY W. BRUDVIG AND VENKAT GOPALAN*

*Electron paramagnetic resonance (EPR) spectroscopy is now part of the armory available to probe the structural aspects of proteins, nucleic acids and protein–nucleic acid complexes. Since the mobility of a spin label covalently attached to a macromolecule is influenced by its microenvironment, analysis of the EPR spectra of site-specifically incorporated spin labels (probes) provides a powerful tool for investigating structure–function correlates in biological macromolecules. This technique has become readily amenable to address various problems in biology in large measure due to the advent of techniques like site-directed mutagenesis, which enables site-specific substitution of cysteine residues in proteins, and the commercial availability of thiol-specific spin-labeling reagents (Figure 1)[1]. In addition to the underlying principle and the experimental strategy, several recent applications are discussed in this review.*

## A. Theory

### *A.1. Introduction to EPR spectroscopy*

If a compound containing unpaired electrons, such as an organic molecule with a free radical, is exposed to an external magnetic field, the energy levels accessible to the unpaired electronic spin are split by that field. Since an electron features a spin of S = 1/2, two energy levels are possible: $M_S = -1/2$, the low-energy state, and $M_S = +1/2$, the high-energy state. As the field strength is increased, the energy difference between these two states increases linearly. This phenomenon

*Roopa Biswas and Venkat Gopalan [E-mail: gopalan.5@osu.edu] are based at the Department of Biochemistry, The Ohio State University, Columbus, OH 43210-1292, USA. Henriette Kühne and Gary Brudvig work at the Department Chemistry, Yale University, New Haven, CT 06520-8107, USA. The current address for Henriette Kühne is The Scripps Research Institute, La Jolla, CA 92037, USA.*

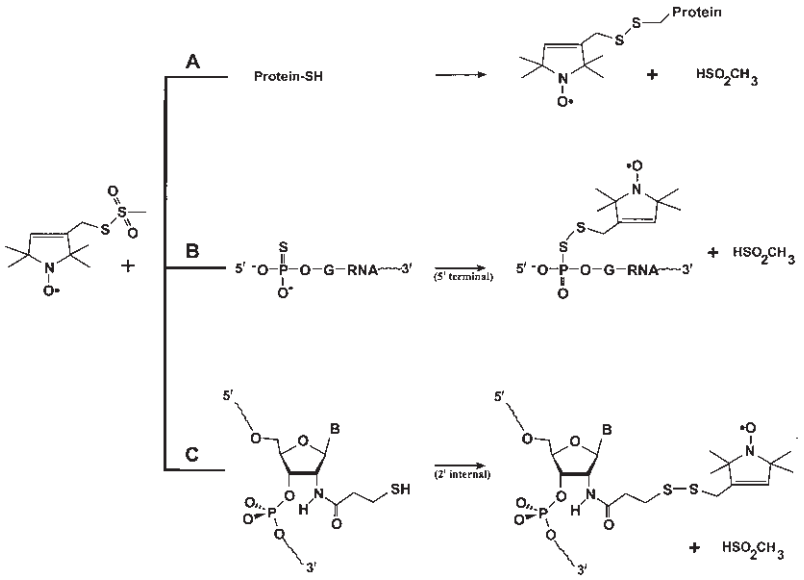


***Fig. 1.*** *Site-directed spin labeling. The covalent attachment of (1-oxyl-2,2,5,5-tetramethyl-$\Delta^3$-pyrroline-3-methyl) methanethiosulfonate (MTS) spin label to a protein (A) or nucleic acid (B, C) is depicted.*

is exploited in EPR spectroscopy, where the compound placed inside the magnetic field is exposed to constant-frequency microwave radiation. At magnetic-field strengths corresponding to an energy difference resonant with the energy of the applied microwave frequency, electrons are promoted from the low-energy to the high-energy state. These transitions are observed as the absorption of a portion of the microwave intensity. Since these absorptions are fairly broad, an accurate measure of the spacing between the peaks is usually obtained by examining the first-derivative spectrum. Therefore, EPR spectra are conventionally recorded as the rate of change of absorption versus field strength (Figure 2).

EPR is a powerful and sensitive technique for the study of macromolecular structure and function because EPR signals are generated only by unpaired electrons, which are fairly rare in biological systems[2,3]. In addition to this fundamental attribute, the widespread use of EPR for investigating biomolecules could also be ascribed to: (1) the influence of the local environment and dynamics of the spin-labeled site on the EPR spectral lineshape; (2) the ease of site-directed spin labeling (SDSL); (3) the absence of size constraints (which is a major limitation in NMR-based approaches to study macromolecular structure); (4) the low molecular volume of the spin

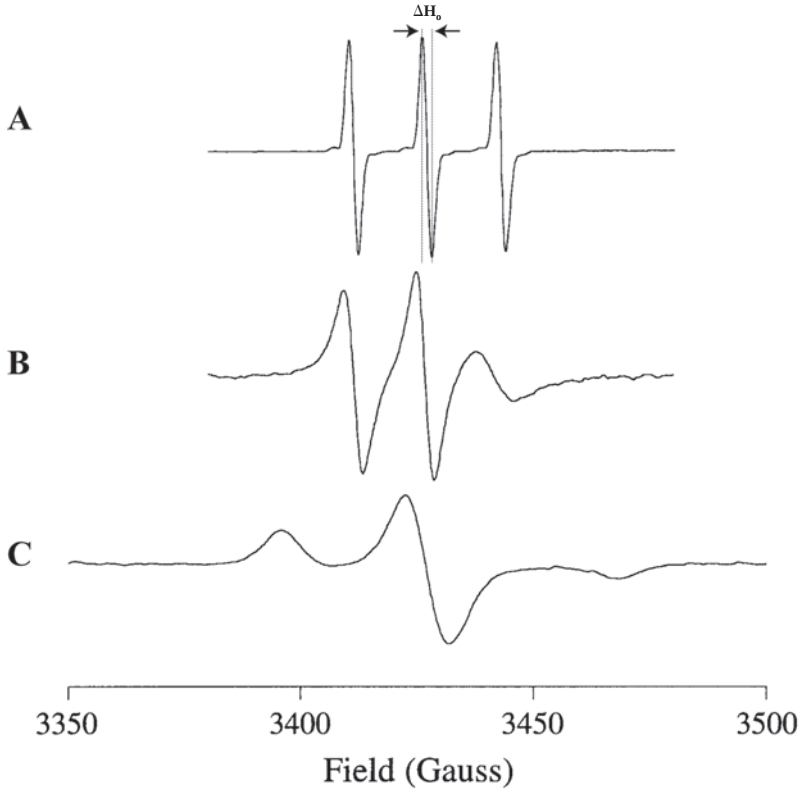


***Fig. 2.*** *Variations in spectral lineshape. EPR spectra of a nitroxide spin label in aqueous solution at room temperature (A), in glycerol at room temperature (B), and frozen in aqueous solution (C). All spectra are scaled to have the same amplitude for the center-field peak and are therefore not scaled with respect to concentration.*

label inducing only modest structural perturbations; and (5) small sample size requirement (~ 0.1 nmole).

## *A.2. Site-directed spin labeling (SDSL)*

The concept of attaching a stable organic radical to a biomolecule as an EPR reporter group was introduced more than thirty years ago[4]. Among the various probes available, nitroxide spin labels have enjoyed widespread use for the study of macromolecular structure and dynamics because they are extremely stable and feature a sharp, well-resolved and simple EPR signal.

The highly stable nitroxide radical is usually incorporated into a heterocyclic ring (such as a pyrrolidine or piperidine) and then covalently attached to a macromolecule via a linker arm (Figure 1); the

length and flexibility of the linker will influence the mobility of the spin label incorporated in the biomolecule. Although spin labeling of proteins can be accomplished through different routes depending on which functional groups in the protein serve as the target for derivatization, thiol-specific spin labeling using alkyl-thiosulfonates remains the most popular on account of their specificity for cysteines and rapid reactivity under mild conditions in buffered aqueous solutions. For example, the commercially available methanethiosulfonate derivative (1-oxyl-2,2,5,5-tetramethyl-$\Delta^3$-pyrroline-3-methyl) methanethiosulfonate (MTS) is covalently attached to a native or engineered Cys residue in a protein via a disulfide bridge (Figure 1A) .

Nucleic acids were spin labeled nearly three decades ago with alkylating agents or by modifying reagents that exploited a unique property such as the presence of 4-thiouridine or an aminoacyl group in a tRNA[1,5–7]. Recent advances such as *in vitro* transcription and solid-phase oligonucleotide synthesis have now made possible sequence/site-specific spin labeling of any RNA or DNA molecule[8]. For instance, the addition of guanosine 5′ monophosphorothioate (GMPS) in an *in vitro* transcription results in enzymatic synthesis of an RNA molecule which could be spin-labeled at its 5′ end. Since GMPS could only substitute for GTP as the initiating nucleotide, the incorporation of GMPS in an RNA molecule positions a unique sulfur at the 5′ terminus which can be spin labeled with MTS (Figure 1B)[8]. Using this approach in conjunction with circular permutation, nitroxide spin labels can be incorporated at any desired position in an RNA molecule. Circular permutation is an elegant approach to create new termini in a molecule. Using the polymerase chain reaction, DNA templates can be generated which when transcribed result in circularly permuted RNAs that are variants of the wild-type molecule in that they possess new 5′ and 3′ termini and their original 5′ and 3′ ends are covalently linked[9]. Several studies indicate that circularly permuted RNAs are comparable to the wild type RNA in terms of their overall structure and function; in fact, this approach has been used effectively to introduce crosslinking reagents as well as spin labels in RNAs[9–11]. In an alternative strategy, a 2′ amine incorporated at a specific site during solid-phase synthesis of a DNA or RNA oligonucleotide could be converted to a thiol-bearing moiety (by treatment with an activated ester and reducing agent), which could then be modified using a MTS derivative (Figure 1C)[12].

Regardless of the labeling procedure, subsequent gel filtration or dialysis procedures are necessary to remove excess, unreacted spin label. Moreover, the modified protein or nucleic acid should always

be tested for functional activity to ensure that the structural perturbation introduced by the spin label is not detrimental for function.

### *A.3. Lineshape analysis: Biological applications*

The rate of rotation (or tumbling) of the spin label influences the lineshape of its EPR spectrum. Therefore, the EPR signal of a spin label covalently tethered to a biomolecule can yield a range of information about its structural environment. Spin labels serve as excellent probes of solvent accessibility, local geometry and flexibility, as well as structural changes induced by a chemical or physical event. Moreover, spin labels can be utilized to measure intra- and intermolecular distances in macromolecular assemblages by dipolar EPR methods.

In the nitroxide spin label, the unpaired electron resides in an orbital associated with the $^{14}N$ nucleus, which has a nuclear spin of $I = 1$. The proximity of this nuclear spin and its three associated quantum states ($M_I = -1$, 0, and 1) leads to further splittings in the possible energy levels, yielding three allowed transitions of equal probability and, consequently, three so-called hyperfine lines in the EPR spectrum of the nitroxide radical (Figure 2A).

If the nitroxide spin label is freely tumbling in solution, it exhibits an isotropic EPR spectrum (Figure 2A). A similar spectrum would be observed if the spin label were attached to a molecule that is sufficiently small or flexible such that the rotational correlation time ($\tau_c$) of the label is less than or comparable to the inverse width of the hyperfine splitting, when the splitting in the associated EPR spectrum is expressed in frequency units. For nitroxide spin labels, this fast averaging limit is below $\tau_c \sim 2$ ns. In contrast, if the mobility of the nitroxide spin label is restricted, a less isotropic EPR lineshape is observed due to the unpaired electron of the nitroxide group residing in a molecular orbital of primarily 2p character along the N–O bond[2]. The highly oriented shape of this orbital favors certain dipole orientations between the electronic spin of the radical and the nitrogen nucleus, leading to an orientation-dependent hyperfine splitting. A label attached to a large molecule with a sufficiently slow $\tau_c$ (> 0.1 ms) will exhibit a broad powder EPR spectrum typical of a completely immobilized sample (Figure 2C). Depending on the degree of spin label immobilization, partially broadened spectra may also be observed indicating mobility on an intermediate time scale (Figure 2B). Generally, broadening of the peaks in an EPR spectrum is indicative of immobilization of the spin label, whereas sharpening of the peaks points to an increase in label mobility. The inverse line width of the central resonance ($\Delta H_o^{-1}$) has frequently been employed

as a measure of the mobility of the spin label[13]. Alternatively, since the amplitudes of the peaks are altered as the peaks broaden, the ratio of the respective peak-to-peak amplitudes observed for both the low-field ($M_I = -1$) and center-field ($M_I = 0$) peaks has also been used to assess the mobility of the spin label.

### *A.3.1. Solvent accessibility and distance measurements in macromolecular complexes*

Interactions with other paramagnetic species can influence the EPR behavior of the spin label[2]. If two paramagnets present in a system are close to each other (< 25 Å), their interaction will influence the EPR behavior of each individual paramagnetic center. This fact can be exploited to study solvent accessibility and measure intra- and inter-molecular distances in macromolecules. The two paramagnetic species used to study dipolar interactions may consist of organic radicals (*e.g.*, nitroxide spin labels), naturally occurring protein radicals (*e.g.*, tyrosyl side chains), or certain transition metal ions (*e.g.*, biologically relevant forms of iron or copper).

To gain information on tertiary structure, dipolar interactions need to be quantitated. EPR transitions saturate as the applied microwave power is increased, causing the rate of excitation to approach the rate of spin relaxation. This phenomenon is known as power saturation and can be quantified as the power required to reach half saturation ($P_{1/2}$). The presence of other paramagnetic species can affect $P_{1/2}$. For example, the presence of a nearby fast-relaxing transition metal ion will enhance the rate at which organic radical electrons relax from the high-energy to the low-energy state, thus increasing the microwave power that can be absorbed before the transition saturates[14]. Similarly, relaxation enhancement can be observed in saturation–recovery experiments, where the transition under study is saturated by a pulse of microwave radiation and the rate of its recovery to the ground state is measured. The interactions that underlie spin relaximetry calculations occur through space and vary with the inverse sixth power of the distance. Inter-spin distances of up to 25 Å can be observed routinely between two organic radicals or an organic radical and a metal-ion center[2,15]. It is noteworthy that the use of spin relaximetry to calculate intra- or inter-molecular distances does not suffer from the orientation ambiguities associated with techniques like fluorescence resonance energy transfer.

The solvent exposure of a nitroxide spin label attached to a Cys residue in a protein can be measured by examining its collision frequency with another paramagnetic reagent [such as nickel(II) ethyl-

enediaminediacetate (NiEDDA) or nickel(II) acetonylacetonate (NiAA)] in solution. The $P_{1/2}$ values for the nitroxide in a protein are measured both in the absence and presence of NiEDDA or NiAA. The increase in $P_{1/2}$ that occurs in the presence of NiEDDA or NiAA is converted into a dimensionless accessibility parameter $\Pi$ that helps compare the collision frequency of the protein-bound nitroxide to a reference compound. There should be qualitative agreement in the patterns of $\Pi$ and $\Delta H_0^{-1}$, the inverse line width of the central resonance. The solvent-accessible nitroxides, which display high $\Pi$ values, are likely to enjoy high mobility which in turn will lead to high $\Delta H_0^{-1}$ values in the first-derivative EPR absorption spectrum. The secondary structure of a protein can be deduced by examining the periodicity of $\Pi$ and $\Delta H_0^{-1}$ values exhibited by nitroxides incorporated individually at every position in the protein (for example, see Section *B.1.1*).

When two spin labels are within ~ 15 Å, interspin dipole–dipole and exchange interactions can produce line broadening, and in some cases resolved splittings, of the EPR spectrum. The dipole-dipole splittings vary with the inverse third power of the distance. By using spectral simulations, the distance between the two labels can be estimated. Such an approach could be used to calculate distances between defined positions in a macromolecule[16]. A detailed discussion of these analyses is beyond the scope of this review, but a forthcoming book is devoted to this topic[17].

### *A.3.2. Detection of structural changes*

Since the EPR lineshape yields information about the mobility and structural environment of a spin label, changes in the spectrum may be observed as structural changes take place. For example, the EPR signal from a nitroxide spin label attached to a small denatured protein (in urea) displays an almost isotropic EPR lineshape, because the limited immobilization of the label is caused by its attachment to the protein backbone and, possibly, any residual protein secondary structure. In contrast, the same spin-labeled protein in its folded state exhibits a much higher degree of spin label immobilization due to constraints imposed by a rigid, native tertiary structure[13,15].

The binding of a cofactor/ligand near the spin-labeled site in an enzyme/receptor might decrease or increase the degree of spin label mobility, as indicated by a broadening or sharpening, respectively, of the EPR lineshape. It is important to note, however, that while differences in the EPR lineshape of a spin label point to changes in the structural environment of the spin label, the cause of these

changes may or may not be located in the immediate proximity of the spin label.

It is possible to follow changes in the EPR spectrum of a spin label as a function of time during processes such as protein folding or cofactor/ligand binding. The progress of a slow event can be monitored by repeatedly recording spectra as the process occurs. Since it usually takes at least 30 seconds to record one complete spectrum, processes occurring faster cannot be monitored by this method. Spectral changes concomitant with rapid processes can be observed in real time by monitoring the signal intensity at one field position over time. For example, as a peak broadens during protein folding, the spectral intensity at its corresponding field position decreases. The time resolution of this method is limited only by the initiation time of the reaction and the data acquisition system employed and can be made to approach the millisecond time scale by using stopped-flow EPR[18].

While the background information provided above suffices for this report, in-depth descriptions of basic EPR theory can be found in an excellent textbook on this subject[3]. Moreover, the structure, incorporation strategies and applications of various spin labels are elaborated lucidly in recent reviews[2,15].

## *B. Applications*

We review findings from selected studies to illustrate the applications of EPR spectroscopy in elucidating protein topography and function, nucleic acid dynamics and protein-nucleic acid interactions[8,19,20].

### *B.1. Mapping protein structure and function*

#### *B.1.1. Determination of secondary structures and topography of proteins*

When a segment of a protein is scanned by SDSL, the EPR accessibility parameter $\Pi$ displays a periodicity that is usually indicative of the secondary structure in that segment. For instance, a solvent-exposed residue in a $\beta$-strand will have a higher $\Pi$ value compared to its neighboring residue which is likely to be buried. Hence, a plot of $\Pi$ versus residue number (corresponding to the $\beta$-strand) will display peaks and troughs with a periodicity of 2.0. Similarly, variations with a periodicity of 3.6 are expected for an $\alpha$-helix.

$\alpha$A-Crystallin is a member of the small heat-shock protein family. It is found in the vertebrate lens where it forms hetero-oligomers with $\alpha$B-crystallins and sequesters damaged proteins presumably by using an oligomeric structure essential for its chaperone activity[21]. In

the absence of structural information, mechanistic insights have been sparse. The secondary structure and the folding pattern of a segment of αA-crystallin containing the putative substrate-binding site were recently investigated by SDSL and EPR spectroscopy[21,22]. A nitroxide spin label was incorporated singly at each of the positions 60 through 120 and the mobility as well as solvent exposure of the spin label at each site analyzed. The secondary structure adopted by this segment of the protein was then deduced from the $\Delta H_o^{-1}$ and π values, which indicate the mobility of the nitroxide-labeled side chains and the solvent accessibility of nitroxides to NiEDDA, respectively. The $\Delta H_o^{-1}$ and Π values exhibit a periodicity of 2.0 in the regions encompassing the residues 84–90, 93–101, and 110–120 and clearly indicate the presence of three β-strands in these regions (Figure 3). The absence of any periodic pattern in the $\Delta H_o^{-1}$ and π values for residues 90–93 and 102–108 is indicative of these residues being in unstructured regions.

To ascertain the relative positioning of the three β-strands in the tertiary structure of αA-crystallin, inter-nitroxide distances were

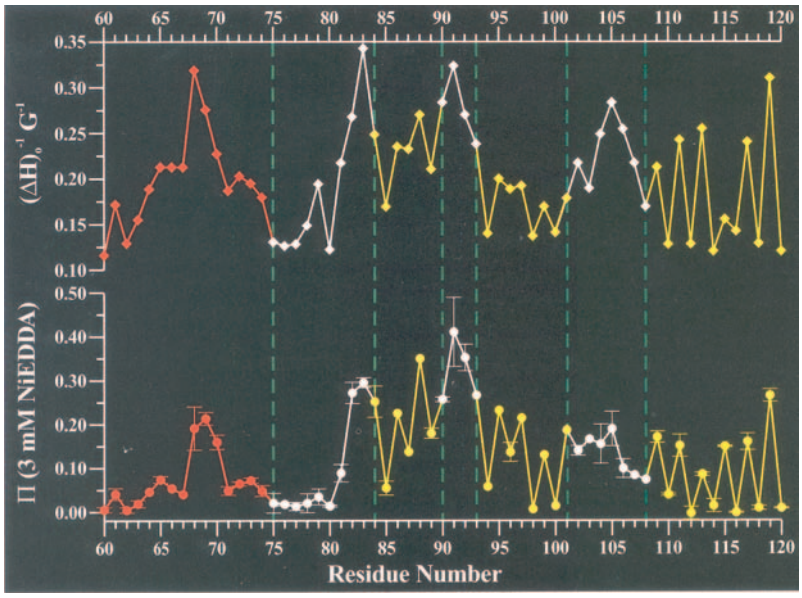


***Fig. 3.*** *Assignment of secondary structure based on $\Delta H_o^{-1}$ and Π values[21]. The segment from 60–120 of αA-crystallin was spin labeled at each position and the mobility ($\Delta H_o^{-1}$) as well as the solvent accessibility (Π) calculated as described in the text[21,22]. Note the periodicity of 2.0 in the regions highlighted by yellow color.*

measured for selected pairs of spin labels introduced in the β-strands of αA-crystallin. The patterns of proximities between various pairs of nitroxides, calculated using dipolar EPR methods, established that the β-strands were arranged in consecutive β-hairpins in an anti-parallel β-sheet[21]. Knowledge of this topology provides a structural basis for understanding substrate binding as well as the chaperone activity of αA-crystallin.

Due to the difficulties inherent in crystallographic studies of membrane proteins, EPR spectroscopy has frequently been employed to obtain information on their secondary structure as well as the topography of individual domains. Studies on lactose (lac) permease and bacteriorhodopsin represent some of the best examples of applications of EPR techniques for mapping protein structure. *Escherichia coli* lac permease is a hydrophobic membrane transport protein that catalyzes the coupled stoichiometric translocation of β-D-galactosides and $H^+$. A wide repertoire of non-crystallographic approaches including EPR spectroscopy have been successfully employed to generate evidence for a helix packing model of the 12-transmembrane helices in lac permease[20,23,24]. These helices are connected by relatively hydrophilic loops with both the N- and C-termini on the cytoplasmic face of the membrane. Helix topographies were identified by EPR studies examining magnetic dipolar interactions either between various pairs of spin-labeled residues or between a bound metal ion (engineered into the protein) and a spin-labeled residue. For instance, a metal-binding site was engineered by mutagenesis (R302H/E325H) in single-Cys lac permease derivatives containing Cys residues in helices II (residues 55–58), V (residues 148 and 150) or VII (residues 233–235)[25]. The EPR spectra obtained in the presence or absence of bound Cu(II) were used to estimate distances between the spin-labeled amino acid residue and the bound Cu(II). The spin–spin interactions indicated a distance of 12–15 Å between Cu(II) and residues 57, 58, 148, 233 and 234. Collectively, the EPR data provided valuable evidence to support the helix packing model and confirmed the proximity of residues which are essential for substrate-binding and catalysis (Figure 4).

Bacteriorhodopsin (bR) is a transmembrane protein which functions as a light-driven proton pump. Based on electron diffraction data, a secondary structure model with seven transmembrane helices was proposed for bR. Since this model was not informative as to the sizes of the helical segments or their relative orientations, spin-label relaximetry was employed to elucidate the transmembrane structure of bR[26,27]. Several single-Cys mutant derivatives of bR were spin labeled and shown to be functional (*i.e.*, light-dependent proton

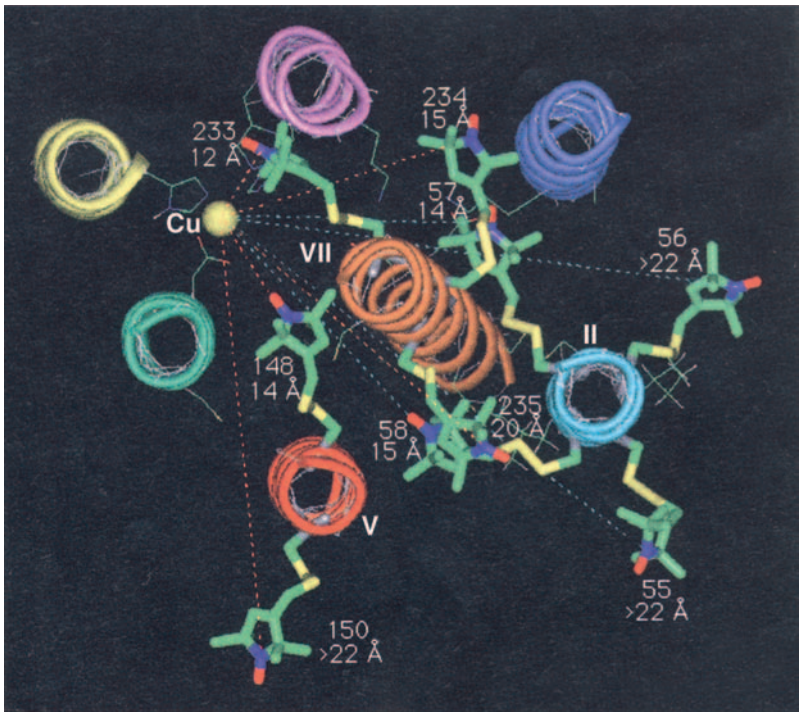


***Fig. 4.*** *Intramolecular distances based on dipolar interactions between a metal-ion center and a nitroxide spin label. A secondary structure representation of lac permease is provided to show interactions between Cu(II) and the various spin-labeled residues. The various helices are indicated by different colors: II (cyan), V (red), VII (brown), VIII (green), IX (yellow), X (pink) and XII (purple), and the Cu(II) ion is indicated by a yellow sphere. The distances obtained between the various nitroxides and Cu(II) are shown by dotted lines*[23].

translocation activity) upon reconstitution into vesicles. Power-saturation EPR spectroscopy was then used to estimate the relative collision frequency of each spin label (at various positions in the vesicle-embedded bR) with membrane-impermeant chromium oxalate (CROX) and freely diffusing oxygen[26,28]. Since CROX is restricted to the aqueous phase, its collisions are restricted to nitroxides attached to solvent-exposed Cys residues. In contrast, oxygen enjoys solubility in the hydrocarbon bilayer and can collide with a spin label in the membrane interior. The periodicity reflected in the accessibility of residues to CROX or oxygen helped establish the length and composition of the transmembrane helices and the loop regions, as well as identify residues at the water-membrane boundary. More-

over, pairs of spin-labeled residues were used to establish the proximity of helices in relation to one another and thereby develop a comprehensive model of the tertiary structure of bR. Indeed, most aspects of this model were borne out by the crystal structure of bacteriorhodopsin[29].

Structural investigations of several other membrane proteins (*e.g.*, diphtheria toxin and aspartate receptor) have also been performed using SDSL together with EPR[30,31]. Due to space limitations, these examples are not discussed here.

### *B.1.2. Conformational changes relevant for protein function*

The advantages of EPR spectroscopy for investigating protein function and dynamics have been illustrated most convincingly with T4 lysozyme, a 164-amino acid globular protein containing two domains connected by a long helix. It catalyzes the cleavage of a glycosidic bond in a bacterial cell-wall polymer containing alternating N-acetylmuramic acid and N-acetylglucosamine residues. Crystallographic studies of wild-type lysozyme and two mutants (I3P and M6I) revealed different conformations of the protein[32]. The structures of the mutant proteins exhibited a hinge bending absent in the wild-type protein, and an opening of the active site by 8 Å as a consequence of the relative rotation of the N- and C-terminal domains about the hinge. EPR spectroscopy was used to test the hypothesis that the wild-type enzyme has a "closed" active site and that the "open" conformation similar to that observed in the I3P or M6I mutants results upon substrate binding[33,34]. Nitroxide spin labels were introduced simultaneously into pairs of Cys residues in the wild-type protein. In each case, one member of the pair was selected from the N-terminal domain (residues 4, 25 and 39) while the other was from a region expected to undergo relative displacement upon hinge bending (residues 60, 61, 64, 71, 109, and 137). Some of the doubly spin-labeled mutants exhibited an EPR spectrum which was considerably broadened or sharpened in the presence of the substrate (Figure 5A). However, the sum of the EPR spectra of the corresponding singly spin-labeled mutants remained unchanged (Figure 5B). Taken together, these findings indicate that the broadening or sharpening observed with the doubly spin-labeled mutants is attributable to intramolecular spin–spin interactions. Quantitative analysis of the spin-spin interactions between the various nitroxide pairs in the absence and presence of substrate revealed that their proximities were indeed altered in the presence of the substrate, presumably due to a substrate-induced conformational change. For

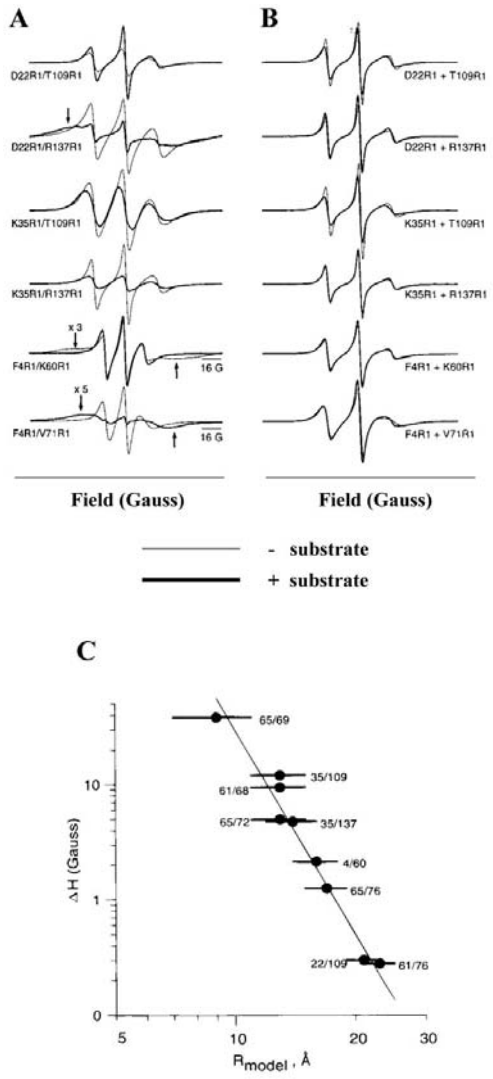


***Fig. 5.*** *Substrate-induced conformational changes in lysozyme. EPR spectra of the doubly spin-labeled cysteine-substituted derivatives (A) and those of the sum of the corresponding individually spin-labeled cysteine-substituted derivatives (B). The spectra obtained in the presence or absence of substrate are shown by a bold or light trace, respectively. (C) A plot of the spin-spin interaction-induced spectral broadening observed in various doubly spin-labeled Cys derivatives of lysozyme versus the interspin distances calculated on the basis of the tertiary structure of lysozyme[34]. The horizontal bars indicate the range of distances determined from molecular modeling.*

instance, substrate binding reduced the distance between residues 22 and 109, and increased the distance between residues 22 and 137 (Figure 5A). Results from this study are consistent with the expectation that the extent of spin-spin interaction-induced spectral broadening decreased with increasing inter-residue distances (Figure 5). Moreover, the inter-spin distances calculated based on magnetic interactions between various nitroxides (attached to Cys residues) correlated remarkably with those observed in the high-resolution crystal structure of lysozyme (Figure 5C). Therefore, the EPR data could be interpreted with confidence to conclude that an 8 Å interdomain movement in lysozyme occurred during the closed- to open-state transition coincident with substrate binding[34].

### *B.1.3. Time-resolved structural changes in proteins*

Stopped-flow experiments were performed to study the kinetics and motional dynamics of specific spin-labeled positions in the water-soluble cytotoxin colicin E1[35]. Specifically, evidence was sought for the hypothesis that two distinct steps occur during the interaction of colicin E1 with membranes. Based on the high-resolution solution structure of colicin A, a structural model of colicin E1 was generated and spin labels were incorporated at positions expected to be solvent exposed or buried in the membrane-bound state. Time-resolved changes in the EPR spectra confirmed the presence of two first-order processes with $t_{1/2}$ values of 6.2 ± 0.4 s and 121 ± 2.4 s, respectively. The EPR data are consistent with a rapid adsorption step and a slow rate-limiting insertion of transmembrane helices in colicin E1 into the membrane interior.

## *B.2. Structures of nucleic acids and nucleic acid-protein complexes*

Structures and dynamics of several nucleic acids and nucleoprotein complexes in solution have been studied using EPR spectroscopy. In these investigations, either spin-labeled nucleic acids were used to study nucleic acid structure (in the absence and presence of their cognate ligands) or spin-labeled proteins were used for elucidating nucleic acid-protein interactions.

### *B.2.1. Nucleic acid structure*

To examine DNA structure and dynamics using EPR spectroscopy, four 15-mer DNA duplexes containing a central AT tract were spin labeled in the major groove at different positions[19]. Spin-labeled nucleic acid building blocks that are acceptable as substrates for

Klenow DNA polymerase were used as part of an elegant chemical and enzymatic synthesis-based approach to incorporate a spin label at specific positions in small DNA molecules[7]. Four modified DNA duplexes were generated, three with the central sequence AATT and were spin labeled at positions 4, 5 and 6 with respect to the dyad axis, while the fourth duplex contained the sequence AAATT and a spin label at position 3 (Figure 6A)[19]. The first three spin-labeled DNA duplexes yielded nearly superimposable EPR spectra. In contrast, the fourth DNA oligomer with the AAA sequence exhibited significant broadening of the EPR lineshape (Figure 6B). Previous studies based on electrophoretic mobility assays have revealed that duplexes containing AAA triplets are structurally distorted due to bending of the DNA helix[36]. Moreover, crystal structures of B-DNA duplexes with AA steps show compression of the major groove[37]. Since the nitroxide spin label was in the major groove of all four 15-mer DNA duplexes, the broadened EPR lineshape of the AAA triplet-containing duplex was ascribed to an increased immobilization of the probe caused by narrowing of the major groove and bending of the duplex.

Crystallographic studies of *E. coli* $tRNA_f^{Met}$ (the initiator tRNA) and yeast $tRNA^{Phe}$ (an elongator tRNA) revealed structural differences at the 3′ end in addition to those observed in the anticodon loop[38]. To establish that the solution structure of these two functionally distinct tRNAs are indeed different, a nitroxide spin label was attached to the 3′ ends of these two tRNAs[39]. The differences in the EPR spectra of these two spin-labeled tRNAs confirm the difference in the micro-environment of their 3′ termini (Figure 7). The spin label at the 3′ terminus of the $tRNA_f^{Met}$ exhibited lower mobility, presumably because it was folded over the aminoacyl stem, whereas that at the 3′ end of the elongator tRNA showed considerable mobility as expected of a flexible 3′ tail.

### *B.2.2. Nucleic acid-protein interactions*

*Eco*R I is a site-specific endonuclease and was one of the first protein molecules to be co-crystallized with its cognate nucleic acid ligand[40]. The latter structure is a paradigm for the study of DNA–protein interactions. Although the high-resolution structure revealed a kink in the substrate DNA helix, it was unclear whether this kink was the result of protein-induced conformational changes. EPR spectroscopy has been used to address this question[41]. Three synthetic 26-mer oligonucleotide sequences with spin labels at positions 6, 9 and 11 (with respect to the dyad axis in GAATTC, the recognition site of *Eco*R I) were prepared for this study. The

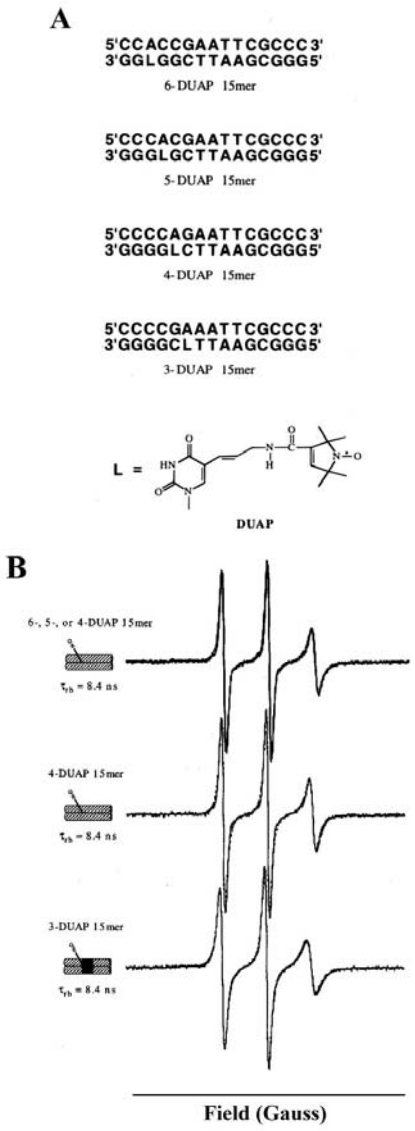


***Fig. 6.*** *DNA structure and dynamics. (A) The oligonucleotide sequences spin labeled with 5-[3-(2,5-dihydro-2,2,5,5-tetramethyl-1-oxyl-1-pyrrole-3-carboxamido)prop-1-enyl]-2′-deoxyuridine (DUAP) at four different positions indicated by "L" (numbering is based on the dyad axis). (B) The EPR spectra of 6-, 5-, and 4-DUAP spin-labeled oligomers (top panel) exhibit near identical lineshape, while the spectrum of the 3-DUAP oligomer containing the triplet AAATT sequence exhibits a broadening in the lineshape (bottom panel). The middle panel is a simulated EPR spectrum for the 4-DUAP spin-labeled oligomer[19].*

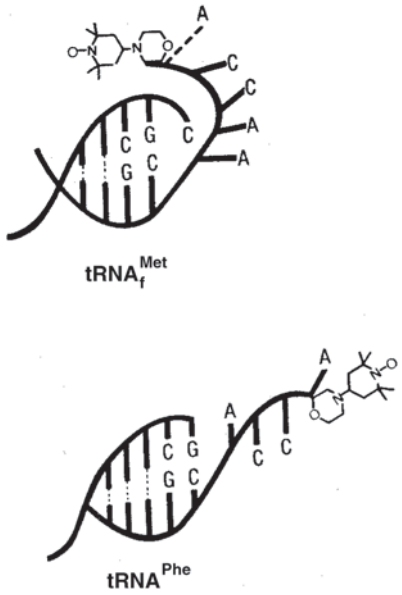


***Fig. 7.*** *Structural variations in tRNAs. Schematic representation of the 3′ termini of the initiator tRNA (tRNA$_f^{Met}$) and an elongator tRNA (tRNA$^{Phe}$). Note that the ACCA in the initiator is folded over the aminoacyl stem while it is free to rotate in the elongator tRNA*[39].

oligomers spin labeled at positions 9 and 11 exhibited no change in the EPR spectra upon addition of the protein. However, the oligomer labeled at position 6 showed broadening of the EPR spectrum, suggesting that distortion of the major groove at this site is induced by *Eco*R I binding.

EPR spectroscopy also allows quantitation of nucleoprotein complex formation in solution under physiological conditions. The DNA binding affinity of bacteriophage fd gene 5 protein has been determined using EPR spectroscopy[42]. The binding study involved titration of the spin-labeled polyA and polyT with the gene 5 protein. An increase in nucleoprotein complex formation was indicated by the corresponding broadening of the EPR spectra. The spectroscopic data were used to calculate the fraction of molecules present as a nucleoprotein complex which in turn yielded the apparent binding constants for formation of this DNA–protein complex.

While SDSL of large nucleic acids remains labor-intensive, it is important to note that nucleic acid–protein interactions can be investigated to a limited extent using spin-labeled proteins and their unlabeled nucleic acid ligands. An example of such an approach involves a study

of ribonuclease P (RNase P), a ubiquitous ribonucleoprotein (RNP) essential for tRNA biosynthesis. *E. coli* RNase P is comprised of a catalytic RNA subunit (M1 RNA, 377 nts) and a protein cofactor (C5 protein, 119 aa residues). To study RNA–protein interactions between the two subunits of RNase P, several single Cys-substituted mutants of C5 protein were modified with MTSL and reconstituted *in vitro* with M1 RNA. The low- and center-field peak amplitude ratios indicated M1 RNA-induced broadening or sharpening of the EPR spectra of the various spin-labeled C5 protein derivatives. In particular, the EPR spectra indicated that residues 16, 54 and 66 of C5 protein are located at or near the M1 RNA-C5 protein interface[43]. These results were not only consistent with previous biochemical studies that identified residues in C5 protein essential for RNase P catalysis but also provided the rationale for footprinting experiments. Cys residues, indicated to be at the RNA-protein interface by EPR spectroscopy, when modified with EDTA-Fe led to a directed hydroxyl radical-mediated footprint and helped identify nucleotides in M1 RNA at the RNA-protein interface in the RNase P holoenyzme[44].

The dipolar EPR method has been used recently to map interactions between an RNA-binding protein and its cognate RNA ligand. In this approach, single spin labels are introduced at unique sites on both the protein and RNA subunits. On evaluating the broadening of the EPR spectra due to the spin–spin splitting that occurs if the two spin-labeled residues interact magnetically, distances between residues on the protein and the bound nucleic acid can be obtained. The interaction between the HIV Rev peptide and the Rev response element (RRE) RNA was studied using this method[8]. The RNA molecule was transcribed *in vitro* in the presence of guanosine 5′ monophosphorothioate, and a thiol-specific nitroxide spin label was introduced at the 5′ end (Figure 1B). The position of the spin label was varied by using three circularly permuted RRE RNAs (RRE1, RRE2, RRE3) with varying 5′ ends (Figure 8A). The Rev peptide was also site-specifically spin labeled at position 51. The EPR spectrum of the reconstituted Rev-RRE RNA complex exhibited a broadened spectrum compared to that observed when either Rev or RRE RNA alone was spin labeled in the reconstituted complex. The overall spectral broadening due to the spin-spin splitting resulting from dipolar interactions was used to obtain interspin distances in the doubly spin-labeled RNP complexes[45]. For instance, the distance calculated from spin–spin splitting when 5′-end spin-labeled RRE1 was reconstituted with Rev peptide spin-labeled at position 51 was 14 Å; this is consistent with the distance of 17 Å determined using the solution structure established by NMR spectroscopy[46] (Figure

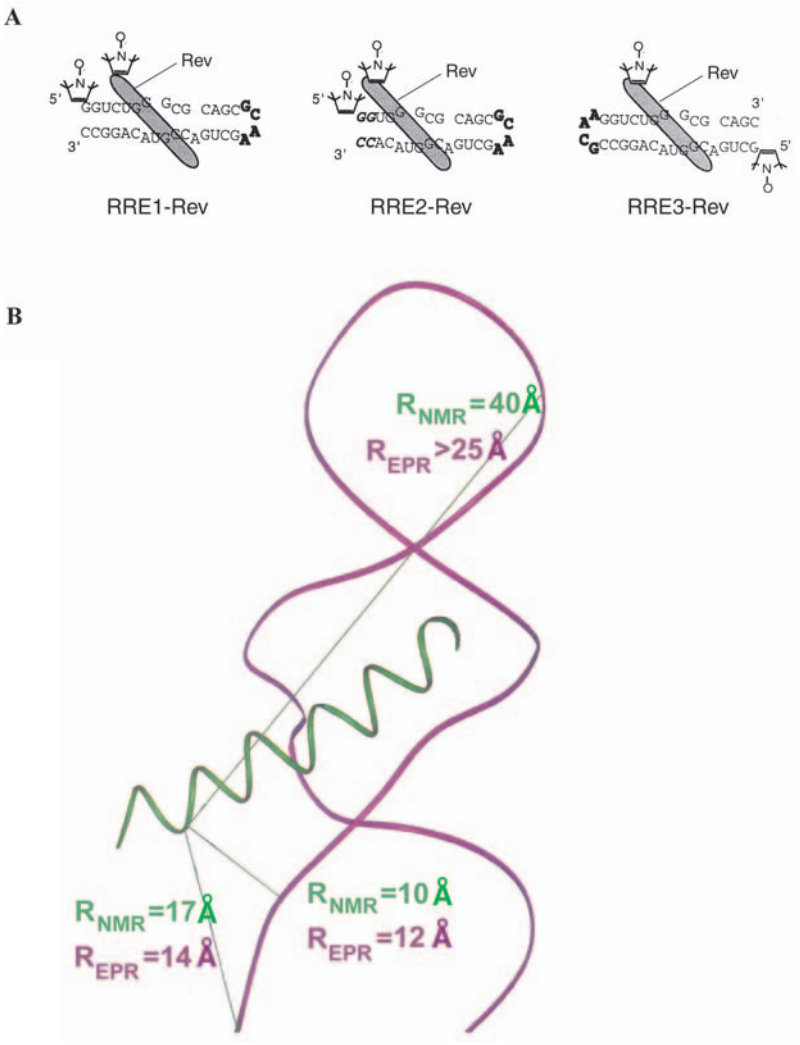


***Fig. 8.*** *RNA–protein interactions in the RRE-Rev complex*[8]*. (A) Schematic representation of the sequence and secondary structure of three circularly permuted RRE RNAs with a spin label at the 5′ end. The spin-labeled Rev peptide bound to the RNA is depicted by a gray rod. (B) The distance between the spin label in the Rev peptide (in green) and those in the RRE RNAs (in purple) were determined by EPR and NMR studies. The distances reported based on the NMR study are calculated using the upper limit for the range of possible Cα-P distances*[46]*.*

8B). There was no broadening due to dipolar effects in the RNP complex reconstituted with spin-labeled RRE3 and Rev indicating that the two spin labels are positioned > 25 Å apart, a conclusion consistent with the distance of 40 Å calculated from the high-resolution structure (Figure 8B). These findings provide a fine illustration of the use of dipolar EPR method for measuring distances in RNP complexes.

## C. Summary

The diverse applications of EPR spectroscopy to study biological macromolecules, where other methods have proven unsuccessful, will ensure its continued use in examining structure–function relationships. EPR spectroscopy is a useful tool to further our understanding even when high-resolution structures are available, since it facilitates studies of internal motions and dynamics of macromolecules in solution.

## Acknowledgements

RB and VG are grateful to the American Heart Association Southern and Ohio Valley Research Consortium for financial support.

## References

1. Bobst, A. M. (1979) Applications of spin labeling to nucleic acids. In: Berliner, L.J. (ed.) *Spin Labeling II–Theory and Applications*, Academic Press, New York, NY.
2. Millhauser, G. L., Fiori, W. R. & Miick, S. M. 1995. Electron spin labels. *Methods Enzymol*., **246**, 589–610.
3. Weil, J. A., Bolton, J. R. & Wertz, J. E. (1994) *Electron Paramagnetic Resonance-Elementary Theory and Practical Applications*. John Wiley & Sons, Inc., New York, NY.
4. Stone, T. J., Buckman, T., Nordio, P. L. & McConnell, H. M. (1965) Spin-labeled biomolecules. *Proc. Natl. Acad. Sci. USA*, **54**, 1010–1017.
5. Hara, H., Horiuchi, T., Saneyoshi, M. & Nichimura, S. (1970) 4-Thiouridine-specific spin-labeling of *E. coli* transfer RNA. *Biochem. Biophys. Res. Commun*. **38**, 305–311.
6. Hilhorst, H. W. M., Postma, U. D. & Hemminga, M. (1982) An EPR study of the kinetics of encapsidation of spin-labeled polyadenylic acid by TMV protein. *FEBS Lett*., **142**, 301–304.
7. Smith, I. C. P. & Yamane, T. (1967) Spin-labeled nucleic acids. *Proc. Natl. Acad. Sci. USA*, **58**, 884–887.
8. Macosko, J. C., Pio, M. S., Tinoco, I. Jr & Shin, Y.-K. (1999) A novel 5′ displacement spin-labeling technique for electron paramagnetic resonance spectroscopy of RNA. *RNA*, **5**, 1158–1166.

9. Harris, M. E. & Christian, E. L. (1999) Use of circular permutation and end modification to position photoaffinity probes for structural analysis of RNA. *METHODS- A companion to Methods in Enzymology*, **18**, 51–59.
10. Nolan, J. M., Burke, D. H. & Pace, N. R. (1993) Circularly permuted tRNAs as specific photoaffinity probes of ribonuclease P RNA structure. *Science*, **261**, 762–765.
11. Thomas, B. C., Kazantsev, A. V., Chen, J.-L. & Pace, N. R. (2000) Photoaffinity cross-linking and RNA structure analysis. *Methods Enzymol*., **318**, 136–147.
12. Cohen S. B. & Cech, T.R. (1997) Dynamics of thermal motions within a large catalytic RNA investigated by cross-linking with thiol-disulfide interchange. *J. Am. Chem. Soc*., **119**, 6259–6268.
13. Hubbell, W. L., Mchaourab, H. S., Altenbach, C. & Lietzow, M. A. (1996) Watching proteins move using site-directed spin-labeling. *Structure* **4**, 779–783.
14. Galli, C., Innes, J. B., Hirsh, D. J. & Brudvig, G. W. (1996) Effects of dipole-dipole interactions on microwave progressive power saturation of radicals in proteins. *J. Magn. Res. Series B*, **110**, 284–287.
15. Hustedt, E. J. & Beth, A. H. (1999) Nitroxide spin-spin interactions: Applications to protein structure and dynamics. *Ann. Rev. Biophys. Biomol. Str*., **28**, 129–153.
16. Budker, V., Du, J.-L., Seiter, M., Eaton, G. R. & Eaton, S. S. (1995) Electron-electron spin-spin interaction in spin-labeled low-spin methemoglobin. *Biophys. J*., **68**, 2531–2542.
17. Eaton, G. R., Eaton, S. S. & Berliner, L. J. (2001) Distance measurements in biological systems by EPR. *Biological Magnetic Resonance*, Vol. 19, Kluwer Academic/Plenum Publishers, New York.
18. Qu, K., Vaughn, J. L., Sienkiewicz A., Scholes, C. P. & Fetrow, J. S. (1997) Kinetics and motional dynamics of spin-labeled yeast iso-1-cytochrome c: 1. Stopped-flow electron paramagnetic resonance as a probe for protein folding/unfolding of the C-terminal helix spin-labeled at cysteine 102. *Biochemistry*, **36**, 2884–2897.
19. Bobst, E. V., Keyes, R. S., Cao, Y. Y. & Bobst, A. M. (1996) Spectroscopic probe for the detection of local DNA bending at an AAA triplet. *Biochemistry*, **35**, 9309–9313.
20. Kaback, H. R., Voss, J. & Wu, J. (1997) Helix packing in polytopic membrane proteins: the lactose permease of *Escherichia coli. Curr. Opin. Struct. Biol*., **7**, 537–542.
21. Koteiche, H. A., Berengian, A. R. & Mchaourab, H. S. (1998) Identification of protein folding patterns using site-directed spin labeling. Structural characterization of a β-sheet and putative substrate binding regions in the conserved domain of αA-crystallin. *Biochemistry*, **371**, 12681–12688.
22. Berengian, A. R., Parfenova, M. & Mchaourab, H. S. (1999) Site-directed spin labeling study of subunit interactions in the αA-crystallin domain of small heat-shock proteins. *J. Biol. Chem*., **274**, 6305–6314.
23. Jung, K., Voss, J., He, M., Hubbell, W. L. & Kaback, H. R. (1995) Engineering a metal binding site within a polytopic membrane protein, the lactose permease of *Escherichia coli. Biochemistry*, **34**, 6272–6277.
24. Kaback, H. R. & Wu, J. (1999) What to do while awaiting crystals of a membrane transport protein and thereafter. *Acc. Chem. Res*., **32**, 805–813.

25. Voss, J., Hubbell, W. L. & Kaback, H. R. (1998) Helix packing in the lactose permease determined by metal-nitroxide interaction. *Biochemistry*, **37**, 211–216.
26. Altenbach, C., Marti, T., Khorana, H. G. & Hubbell, W. L. (1990) Transmembrane protein structure: spin labeling of bacteriorhodopsin mutants. *Science*, **248**, 1088–1092.
27. Steinhoff, H.-J., Mollaaghababa, R., Altenbach, C., Khorana, H. G. & Hubbell, W. L. (1995) Site-directed spin labeling studies of structure and dynamics in bacteriorhodopsin. *Biophys. Chem*., **56**, 89–94.
28. Altenbach, C., Greenhalgh, D. A., Khorana, H. G. & Hubbell, W. L. (1994) A collision gradient method to determine the immersion depth of nitroxides in lipid bilayers: Application to spin-labeled mutants of bacteriorhodopsin. *Proc. Natl. Acad. Sci.USA*, **91**, 1667–1671.
29. Pebay-Peyroula, E., Rummel, G., Rosenbusch, J. P. & Landau, E. M. (1997) X-ray structure of bacteriorhodopsin at 2.5 angstroms from microcrystals grown in lipidic cubic phases. *Science* **277**, 1676–1681.
30. Danielson, M. A., Bass, R. B. & Falke, J. J. (1997) Cysteine and disulfide scanning reveals a regulatory α-helix in the cytoplasmic domain of the aspartate receptor. *J. Biol. Chem*., **272**, 32878–32888.
31. Oh, K. J., Zhan, H., Cui, C., Hideg, K., Collier, R. J. & Hubbell, W. L. (1996) Organization of diphtheria toxin T domain in bilayers: a site-directed spin labeling study. *Science*, **273**, 810–812.
32. Faber, H. R. & Matthews, B. W. (1990) A mutant T4 lysozyme displays five different crystal conformations. *Nature*, **348**, 263–266.
33. Mchaourab, H. S., Lietzow, M. A., Hideg, K. & Hubbell, W. L. (1996) Motion of spin-labeled side chains in T4 lysozyme. Correlation with protein structure and dynamics. *Biochemistry*, **35**, 7692–7704.
34. Mchaourab, H. S., Oh, K. J., Fang, C. J. & Hubbell, W. L. (1997) Conformation of T4 lysozyme in solution. Hinge-bending motion and the substrate-induced conformational transition studied by site-directed spin labeling. *Biochemistry*, **36**, 307–316.
35. Shin, Y.-K., Levinthal, C., Levinthal, F. & Hubbell, W. L. (1993) Colicin E1 binding to membranes: time-resolved studies of spin-labeled mutants. *Science*, **259**, 960–963.
36. Hagerman, P. J. (1985) Sequence dependence of the curvature of DNA: a test of the phasing hypothesis. *Biochemistry*, **24**, 7033–7037.
37. Young, M. A., Ravishanker, G., Beveridge, D. L. & Berman, H. M. (1995) Analysis of local helix bending in crystal structures of DNA oligonucleotides and DNA-protein complexes. *Biophys. J*., **68**, 2454–2468.
38. Woo, N. H., Roe, B. A. & Rich, A. (1980) Three-dimensional structure of *Escherichia coli* initiator $tRNA_f^{Met}$. *Nature*, **286**, 346–351.
39. Pscheidt, R. H. & Wells, B. D. (1986) Different conformations of the 3' termini of initiator and elongator transfer ribonucleic acids. *J. Biol. Chem*., **216**, 7253–7256.
40. Frederick, C. A., Grable, J., Melia, M., Samudzi, C., Jen-Jacobson, L., Wang, B.-C., Greene, P., Boyer, H. W. & Rosenberg, J. M. (1984) Kinked DNA in crystalline complex with *Eco*R I endonuclease. *Nature*, **309**, 327–331.
41. Keyes, R. S., Cao, Y. Y., Bobst, E. V., Rosenberg, J. M. & Bobst, A. M. (1996) Spin-labeled nucleotide mobility in the boundary of the *Eco*R I endonuclease binding site. *J. Biomol. Struct. Dyn*., **14**, 163–172.

42. Bobst, A. M., Ireland, J. C. & Bobst, E. V. (1982) Nucleic acid binding affinity of fd gene 5 in the cooperative binding mode. *J. Biol. Chem*., **259**, 2130–2134.
43. Gopalan, V., Kühne, H., Biswas, R., Li., H., Brudvig, G. W. & Altman, S. (1999) Mapping RNA-protein interactions in ribonuclease P from *Escherichia coli* using electron paramagnetic resonance spectroscopy. *Biochemistry*, **38**, 1705–1714.
44. Biswas, R., Ledman, D. W., Fox, R. O., Altman, S. & Gopalan, V. (2000) Mapping RNA-protein interactions in ribonuclease P from *Escherichia coli* using disulfide-linked EDTA-Fe. *J. Mol. Biol*., **296**, 19–31.
45. Rabenstein, M. D. & Shin, Y.-K. (1995) Determination of the distance between two spin labels attached to a macromolecule. *Proc. Natl. Acad. Sci. USA*, **92**, 8239–8243.
46. Battiste, J. L., Mao, H., Rao, S. N., Tan, R., Muhandiran, D. R., Kay, L. E., Frankel, A. D. & Williamson, J. R. (1996) αHelix-RNA major groove recognition in an HIV-1 rev peptide-RRE RNA complex. *Science*, **273**, 1547–1551.